Neuropsychopharmacology www.nature.com/npp

ARTICLE

The effects of FAAH inhibition on the neural basis of anxiety-related processing in healthy male subjects: a randomized clinical trial

Martin P. Paulus[1,2], Murray B. Stein[1,3], Alan N. Simmons[1,4], Victoria B. Risbrough[1,4], Robin Halter[5] and Sandra R. Chaplan[5]

Acute pharmacological inhibition of the anandamide-degrading enzyme, fatty acid amide hydrolase (FAAH), prolongs the regulatory effects of endocannabinoids and reverses the stress-induced anxiety state in a cannabinoid receptor-dependent manner. However, the neural systems underlying this modulation are poorly understood. A single site, randomized, double-blind, placebo-controlled, parallel study was conducted with 43 subjects assigned to receive once daily dosing of either placebo ($n = 21$) or JNJ-42165279 (100 mg) ($n = 22$) for 4 consecutive days. Pharmacodynamic effects were assessed on the last day of dosing and included evaluation of brain activation patterns using BOLD fMRI during an (1) emotion face-processing task, (2) inspiratory breathing load task, and (3) fear conditioning and extinction task. JNJ-42165279 attenuated activation in the amygdala, bilateral anterior cingulate, and bilateral insula during the emotion face-processing task consistent with effects previously observed with anxiolytic agents. Higher levels of anandamide were associated with greater attenuation in bilateral anterior cingulate and left insula. JNJ-42165279 increased the activation during anticipation of an aversive interoceptive event in the anterior cingulate and bilateral anterior insula and right inferior frontal cortex. JNJ-42165279 did not affect fear conditioning or within-session extinction learning as evidenced by a lack of differences on a subjective and neural circuit level. Taken together, these results support the hypothesis that JNJ-42165279 at this dose shares some effects with existing anxiolytic agents in dampening response to emotional stimuli but not responses to conditioned fear.

Neuropsychopharmacology (2021) 46:1011–1019; https://doi.org/10.1038/s41386-020-00936-w

INTRODUCTION

Anxiety disorders are the most common mental health problem [1], with a lifetime prevalence of ~33% [2]. Anxiety disorders are the sixth leading cause of disability world-wide and show no signs of reduced burden over recent years [3]. Unfortunately, existing treatments are only partially effective for most patients (e.g., [4, 5]), which further exacerbates the cost and suffering associated with these disorders. The endocannabinoid (eCB) system is considered an integral regulator of the stress response [6]. Stress down-regulates cannabinoid type 1 (CB1) receptors, reduces anandamide (arachidonoylethanolamine, AEA), and increases 2-arachidonoyl glycerol [7]. Several investigators have proposed that eCB signaling seems to determine the value of aversive stimuli and thereby helps to tune adaptive behavioral responses, which are essential for the organism's long-term viability, homeostasis, and stress resilience [8]. Interestingly, the eCB system intersects at the hypothalamic–pituitary axis with the CRF-containing nerve fibers [9]. Thus, targeting the eCB system represents an attractive and novel approach to the treatment of anxiety- and stressor-related disorders such as posttraumatic stress disorder (PTSD) [10].

Acute pharmacological inhibition of the anandamide-degrading enzyme, fatty acid amide hydrolase (FAAH) acts to prolong the regulatory effects of the eCB and reverses the stress-induced anxiety state in a cannabinoid receptor-dependent manner [11]. Mice deficient in FAAH are resistant to stress-induced changes in amygdala structure and function [12] and several animal studies show that activation of CB1 receptors reduces fear expression [13, 14]. Kathuria et al. [15] showed that FAAH inhibitors URB597 and URB532 evoked anxiolytic responses in the elevated zero-plus maze and the ultrasonic rat pup vocalization test. FAAH inhibitors prevent stress-induced reductions in AEA and associated increases in basolateral amygdala dendritic hypertrophy and anxiety-like behavior. Additionally, inhibition of FAAH facilitates long-term fear extinction and rescues deficient fear extinction in rodent models [13] and in humans [16]. Finally, others [15, 17] reported that the FAAH inhibitor PF-3845 decreased mouse marble burying. Therefore, it has been hypothesized that inhibition of FAAH and the resulting accumulation of fatty acid amides may have anxiolytic effect in humans, which may be due to accumulation of eCBs acting on the CB1 cannabinoid receptor. Moreover, it has been proposed this mechanism may be particularly useful in the treatment of disorders marked by fear responses that are difficult to extinguish, e.g., memories of a traumatic event in PTSD [18, 19]. Taken together, these studies provide a basis for testing whether a FAAH inhibitor could be useful in the treatment of anxiety and stressor-related disorders [20].

[1]Department of Psychiatry, University of California San Diego, La Jolla, CA, USA; [2]Laureate Institute for Brain Research, Tulsa, OK, USA; [3]Herbert Wertheim School of Public Health and Human Longevity Science, University of California San Diego, La Jolla, CA, USA; [4]VA Center of Excellence for Stress and Mental Health, La Jolla, CA, USA and [5]Janssen Research & Development, LLC, San Diego, CA, USA
Correspondence: Martin P. Paulus (mpaulus@laureateinstitute.org)

Received: 27 August 2020 Revised: 5 November 2020 Accepted: 30 November 2020
Published online: 17 December 2020

The development of new therapeutics based on neuroscience approaches to understand the pathophysiology of these illnesses has stalled [21]. The National Institute of Mental Health began the Research Domain Criteria (RDoC) project in 2009 to develop a research classification system for mental disorders based upon neurobiology and observable behavior [22]. Negative affect systems are dimensions of psychopathology identified by the RDoC work groups [23, 24], with acute threat (fear) and potential harm (anxiety) central constructs within the negative valence system. One approach to measuring response to threat is via fear conditioning, which involves excitatory learning of CS-US associations [25, 26]. Research on fear learning uniquely adapts to translational neuroscience contexts because we understand with great precision the relevant neural processes in many species, including humans. The brain regions that have most consistently been associated with fear conditioning are the amygdala [27–31] and insular cortex [32]. Increased activity in the amygdala and insula are typically observed in response to the CS during conditioning. A second approach to measuring threat is via unconditioned affective/arousal response. One approach to measure unconditioned affective/arousal response is to present emotional faces to participants and have them discriminate the emotional expression [33]. This type of task is associated with an increased amygdala and insula activation during viewing of fearful faces and is consistently associated with increased anxiety symptoms across mood and anxiety disorders [34]. Threat circuit activation during emotional face processing is also highly sensitive to anxiolytic medications [35]. Another domain—less explored by the RDoC approach but highly relevant for anxiety-related processing [36]—is interoception, which comprises receiving, processing, and integrating body-relevant signals together with external stimuli to affect motivated behavior [37, 38]. Interoception circuits comprise peripheral receptors [39], c-fiber afferents, spino-thalamic projections, specific thalamic nuclei, posterior and anterior insula as the limbic sensory cortex, and anterior cingulate cortex (ACC) as the limbic motor cortex (for reviews see [40, 41]). Interoception is sensitive to cannabis, which may play a role in its anxiolytic effects [42].

JNJ-42165279 is an aryl piperazinyl urea inhibitor of FAAH, which is highly selective with regard to other enzymes, ion channels, transporters, and receptors [43]. This study applied functional magnetic resonance imaging (fMRI) using blood-oxygen-level-dependent (BOLD) contrasts to characterize the effects of FAAH inhibition with JNJ-42165279 on three behavioral tasks in healthy male volunteers. Specifically, we used an emotion face-processing task, an inspiratory breath load task which elicits acutely aversive interoceptive sensations [44], and a fear conditioning and extinction task, which has been shown to robustly activate the neural pathways implicated in these processes [45]. The primary objective was to determine whether JNJ-42165279 100 mg administered once daily over 4 days affects fMRI BOLD signals in the amygdala elicited by an emotion face-processing task. The secondary objective was to determine whether this drug affects fMRI BOLD signals in the amygdala, during the extinction phase of a fear conditioning task and the insula, elicited by an inspiratory breathing load task. We hypothesized that JNJ-42165279 administration would be associated with reduced fMRI BOLD signals in these target regions.

METHODS

Study overview

This study was approved by the UCSD IRB (protocol number 130116), each individual participating in this study signed an informed consent and all adverse effects were reported to the UCSD IRB. A previous Phase 1 study conducted by the sponsor included 29 healthy male subjects to evaluate the safety, pharmacokinetics, and pharmacodynamic activity. Thus, the sponsor suggested to recruit males only for this single site, randomized by a prespecified number code, double-blind, placebo-controlled, parallel study (detailed study procedure can be found in the Supplementary and time and events Supplementary Table 1). Forty-three subjects were randomly assigned to receive once daily dosing of either placebo or JNJ-42165279 (100 mg) for 4 consecutive days to achieve a steady-state level. The dose was chosen because a single dose of 100 mg resulted in over 90% inhibition of FAAH activity in WBC for about 24 h and the 4-day steady-state design was chosen based on prior studies by the sponsor that showed mean terminal half-life values for doses between 10 and 250 mg of 8.6 to 14 h, supporting the idea that steady-state concentrations would be reached by the third day of repeated administration. Subjects visited the clinic on each of the 4 days at which time the study drug was administered orally by designated study personnel at the study site. Pharmacokinetic data and more detail about the compound are available in the Supplementary. There was a clear separation of mean N-arachidonoylethanolamine, N-palmitoylethanolamide, and N-oleoylethanolamide plasma concentrations between the FAAH inhibitor and the placebo group (Supplementary Figs. 1 and 2). Pharmacodynamic effects were assessed on the last day of dosing and included evaluation of brain activation patterns using BOLD fMRI during (1) emotion face-processing task (2) inspiratory breathing load task, and (3) fear conditioning and extinction. The effects were assessed in a-priori identified emotional brain neurocircuitry consisting of (a) bilateral amygdala, (b) bilateral insula, (c) bilateral medial prefrontal cortex (mPFC), and (d) ACC. Questionnaires were used to evaluate changes in mood, and blood biomarkers of FAAH inhibition were measured. A safety follow-up visit occurred 7–14 days after administration of the last dose of study drug.

Subjects

Male participants between 18 and 45 years of age with a body mass index between 18 and 30 kg/m^2, who were in good general health and exhibited sufficient proficiency in English language to understand and complete interviews, questionnaires, and all other study procedures were recruited between August 2013 and August 2014. Sexually active males were required to agree to use a condom during the study and for 3 months after receiving the last dose of study drug. Each subject was genotyped and the results with respect to rs324420 SNP are provided in the Supplementary Table 2 and Supplementary Fig. 3. Exclusion criteria consisted of: (1) history of liver or renal insufficiency; glaucoma; significant cardiac, vascular, pulmonary, gastrointestinal, endocrine, neurologic, hematologic, rheumatologic, or metabolic disturbance; or any other condition that, in the opinion of the investigator, would make participation not be in the best interest of the subject or that could prevent, limit, or confound the protocol-specified assessments; (2) met DSM IV criteria for any Axis I disorder; (3) had contraindication(s) to MRI, (4) had active suicidal ideation; (5) had a history (including family) of motor tics or diagnosis of Tourette's syndrome; (6) had recurrent severe headache or migraine, fainting spells, or seizures, or has a history of severe traumatic brain injury; (7) had a history of malignancy within 5 years before screening; (8) had corrected QT interval greater than 445 ms at screening; (9) had smoked an average of more than five cigarettes per day over the past month; (10) had known allergies, hypersensitivity, or intolerance to hypromellose (suspension for the drug administration); (11) had used prohibited concomitant therapy prior to the planned first dose; (12) had received an investigational drug or used an invasive investigational medical device within 1 month or a period less than 5 times the drug's half-life; (13) had a positive test for drugs of abuse, including cannabis, at screening or Day 1; (14) had a positive test for human immunodeficiency virus, hepatitis B, or hepatitis C; (15) had substance or alcohol dependence within the past year; (16) had habitual caffeine consumption of more than 400 mg/d.

Procedures

Emotion face-processing task. During fMRI, each subject was tested on a modified [35] version of the emotion face-processing task, which is described in detail here [46].

Inspiratory breathing load task. Participants completed a well-validated inspiratory breathing load fMRI paradigm [47]. (for details see Supplementary). The main dependent measures of interest were reaction time (RT), accuracy, and brain activation during the anticipation, breathing load, and postbreathing load conditions relative to the baseline condition.

Fear conditioning/extinction task (based on a task by Sehlmeyer et al. [45, 48]). Prior to scanning, detailed task instructions were given and participants were familiarized with the task. In a differential conditioning paradigm, pictures of two different fractal stimuli served as conditioned stimuli (CS−, CS+). The experiment was divided into three phases. (1) during habituation, each CS was shown five times without US. (2) During each of the two acquisition phases the subject saw 15 CS−, 15 CS+ without US (CS+ unpaired) and five CS+ with US (CS+ paired) trials. In this 25% partial reinforcement schedule, the unconditioned stimulus (US) was a loud scream. (3) In the extinction phase, 25 CS+ unpaired and 25 CS– trials were presented (details are described in the Supplementary).

Image analysis

Acquisition of images. All scans were performed on a 3T GE CXK4 Magnet (General Electric Medical. Systems, Milwaukee, WI) at the UCSD Keck Imaging Center, which is equipped with eight high-bandwidth receivers that allow for shorter readout times and reduced signal distortions and ventromedial signal dropout. Each 1-h session consisted of a 3-plane scout scan (10 s), a standard anatomical protocol (i.e., a sagittally acquired spoiled gradient recalled sequence) (FOV = 25 cm, matrix = 192 × 256 (extrapolated to 256 × 256), 172 sagittally acquired slices 1-mm thick, TR = 8 ms, TE = 3 ms, flip angle = 12°. We used an 8-channel brain array coil to axially acquire T2*-weighted echo-planar images (EPIs) with the following parameters: FOV = 23 cm, matrix = 64 × 64, 30 slices 2.6-mm thick, gap = 1.4 mm, TR = 2000 ms, TE = 32 ms, flip angle = 90°.

Image analysis pathway. The basic structural and functional image processing were conducted with the Analysis of Functional NeuroImages (AFNI) software package [49]. A multivariate regressor approach described below was used to relate changes in EPI intensity to differences in task characteristics [50]. EPIs were coregistered using a 3D-coregistration algorithm [51] that has been developed to minimize the amount of image translation and rotation relative to all other images. Six motion parameters were obtained for each subject. Three of these motion parameters were used as regressors to adjust for EPI intensity changes due to motion artifacts. All slices of the EPI scans were temporally aligned following registration to ensure that different relationships with the regressors were not due to the acquisition of different slices at different times during the repetition interval.

Multiple regressor analyses. The details of these analyses have been described elsewhere [35, 47, 52]. *Emotion face-processing task*: four regressors of interest were (1) happy, (2) angry, (3) fearful, and (4) circle/oval (i.e., shape) sensorimotor condition. These 0–1 regressors were convolved with a gamma variate function [53] modeling a prototypical hemodynamic response (6–8 s delay) [54] and to account for the temporal dynamics of the hemodynamic response (typically 12–16 s) [55]. The convolved time series was normalized and used as a regressor of interest. A series of regressors of interest and the motion regressors were entered into the AFNI program 3dDeconvolve to determine the height of each regressor for each subject. The main dependent measure was the voxel-wise normalized relative signal change (or percent signal change for short), which was obtained by dividing the regressor coefficient by the zero-order regressor. Spatially smoothed (4-mm full-width half-maximum Gaussian filter) percent signal change data were transformed into Talairach coordinates based on the anatomical magnetic resonance images, which was transformed manually in AFNI. *Inspiratory breathing load task*: regressors of interest were generated to delineate conditions (anticipation, breathing load, post anticipation, and postbreathing load). To that end, a 0–1 reference function of the particular time interval for each condition was convolved with a gamma variate function. Six movement regressors, a baseline and linear drift regressor, and normalized regressors of interest (anticipation, breathing load, post anticipation, postbreathing load), were included in the AFNI program 3dDeconvolve to estimate the goodness of fit between model estimates and BOLD responses for each subject. The baseline condition, wherein participants were performing the CPT but not experiencing anticipation, breathing load, post anticipation, or postbreathing load conditions, served as the baseline for this analysis. *Fear conditioning/extinction task*: individual time series data were then analyzed with AFNI's *3dDeconvolve* program to generate activation at each voxel. Regressors of noninterest included motion parameters, linear drift, CS+ paired trials, and the continuous performance task (subject-specific regressor modeling the RT for each button press). Regressors of interest modeled CS+ unpaired and CS− image presentation periods. The result of this analysis yielded activation for each participant to the CS+ and CS− during acquisition and extinction, with each phase broken into early and late halves.

Statistical analysis

The voxel-wise Talairach-transformed % signal change data was the main dependent measure. For example, for the breathing load fMRI paradigm the dependent measure was the % signal change during anticipation, stimulation, and poststimulation period, respectively. These dependent measures were entered into a linear mixed effects model [56]. We use the implementation of the linear mixed effects models in R [57], which estimates the parameters of the mixed model using Maximum Likelihood Estimation (MLE) or Restricted MLE (RMLE) procedures. A mixed ANOVA model was computed for the Linear Mixed Effects model to obtain the numerator degrees of freedom, denominator degrees of freedom, *F* values, and *P* values for Wald tests for the terms in the model. These calculations were completed within the R computing environment using routines that read in AFNI data sets. Specifically, the experimental condition (e.g., anticipation, stimulation, poststimulus interval) was used as fixed factor and subject was used as a random factor. The hypothesized effects were estimated using specific contrast matrices. Monte–Carlo simulations were conducted to guard against identifying false positive areas of activation. Based on simulations implemented in the recently corrected AFNI program 3dClustSim (using spatial Auto-Correlation-Function as derived by 3dFWHMx), a voxel-wise a-priori probability of 0.01 will result in a corrected cluster-wise probability of 0.05 if the cluster has a minimum volume of prespecified volumes for each region of interest. Only these clusters were considered for ROI analyses.

RESULTS

A total of 43 healthy men were randomized and received at least 1 dose of JNJ-42165279 ($n = 22$) or placebo ($n = 21$). All randomized and treated subjects were included in the pharmacodynamic analysis set and the safety analysis set. Forty-one subjects (95.3%) completed the study. Two subjects were withdrawn from the study early: one subject in the placebo group was withdrawn due to an adverse event (increase in creatine phosphokinase) and one subject in the JNJ-42165279 group was withdrawn due to a

Table 1. Demographic and baseline characteristics.

	Placebo	JNJ-42165279	Total
Age (years)			
N	21	22	43
Mean (SD)	22.1 (3.03)	23.3 (3.59)	22.7 (3.35)
Median	22.0	22.5	22.0
Range	(18; 28)	(18; 32)	(18; 32)
Gender			
N	21	22	43
Male	21 (100.0%)	22 (100.0%)	43 (100.0%)
Female	0	0	0
Race			
N	21	22	43
White	13 (61.9%)	11 (50.0%)	24 (55.8%)
Black or African American	0	2 (9.1%)	2 (4.7%)
Asian	2 (9.5%)	7 (31.8%)	9 (20.9%)
American Indian or Alaska Native	1 (4.8%)	0	1 (2.3%)
Native Hawaiian or Other Pacific Islander	3 (14.3%)	0	3 (7.0%)
Other	1 (4.8%)	2 (9.1%)	3 (7.0%)
Baseline Weight (kg)			
N	21	22	43
Mean (SD)	76.4 (10.45)	76.5 (10.39)	76.4 (10.30)
Median	76.2	76.1	76.2
Range	(57; 101)	(62; 98)	(57; 101)
Baseline BMI (kg/m^2)			
N	21	22	43
Mean (SD)	24.16 (2.549)	24.11 (2.964)	24.14 (2.736)
Median	24.00	24.65	24.50
Range	(19.0; 28.6)	(18.0; 29.2)	(18.0; 29.2)
Handedness			
N	21	22	43
Left-handed	3 (14.3%)	4 (18.2%)	7 (16.3%)
Right-handed	18 (85.7%)	17 (77.3%)	35 (81.4%)
Ambidextrous	0	1 (4.5%)	1 (2.3%)

Percentages calculated with the number of subjects per parameter in each group as denominator.

protocol deviation. One subject in the JNJ-42165279 group completed the MRI assessment but was excluded from the analysis of the imaging data due to technical difficulties with the data transfer; this subject was however included in the analysis of the behavioral data.

Demographic and baseline characteristics were generally comparable between the JNJ-42165279 and placebo treatment groups (Table 1). The mean age of the subjects was 22.7 years (range: 18–32 years) and mean body mass index was 24.1 kg/m^2 (range: 18.0–29.2 kg/m^2). Most subjects were right-handed; 4 (18.2%) subjects in the JNJ-42165279 group and 3 (14.3%) subjects in the placebo group were left-handed.

Emotion face-processing task

No statistically significant differences were observed between the JNJ-42165279 and placebo groups in performance accuracy or RT for any of the conditions (shapes, angry faces, fearful faces, happy faces), or across conditions (see Supplementary Table 3). Performance accuracy was near 100% for both treatment groups during all conditions. While no statistical comparison was performed, RTs were longer during the face conditions than during the shape condition.

Mean BOLD fMRI Talairach-transformed percent signal changes in the amygdala (the primary region of interest in this analysis) and other regions of interest (ACC and insular cortex) during the emotion face-processing task across each of the three conditions (fearful faces, happy faces, and angry faces) revealed a significant effect of drug. Seven subregions (left parahippocampal gyrus, left/right anterior cingulate, left/right medial frontal gyrus, left/right insula) were identified as showing a statistically significant between-group difference across conditions within the search regions of interest. Mean BOLD fMRI Talairach-transformed percent signal changes in these seven subregions and the estimated between-group differences are shown Table 2. As shown in Fig. 1, JNJ-42165279 attenuated activation regardless of face valence. Moreover, those individuals treated with JNJ-42165279 that showed the greatest increase in plasma AEA at day 4 also showed the greatest reduction in BOLD fMRI activation in left/right anterior cingulate, and left insula (Supplementary Fig. 4).

Breathing load task

There were no statistically significant between-group differences observed for performance accuracy or RT during the breathing load task for any condition (i.e., anticipation, stimulation, post stimulation; Supplementary Table 4). Accuracy was near 100% in both treatment groups throughout the task. While no statistical comparison was performed, RTs appeared higher during the poststimulation condition compared with the other conditions.

At the pre-MRI assessment, no statistically significant differences were observed between the JNJ-42165279 and placebo groups for ratings of pleasantness, unpleasantness, or intensity. At the post-MRI assessment, the pleasantness rating was statistically significantly lower in the JNJ-42165279 group than in the placebo group ($p = 0.0449$). No between-group difference was observed for the rating of intensity (see Supplementary Table 5).

Mean BOLD Talairach-transformed percent signal changes in the bilateral insula (primary region of interest for this analysis) and the other regions of interest (amygdala and ACC) during the breathing load task were obtained for the three conditions (anticipation, stimulation, post stimulation) and are summarized in Supplementary Table 6. Four subregions (right anterior cingulate, left/right insula, and right inferior frontal gyrus) were identified as showing a statistically significant between-group difference during the anticipation condition; no subregions were identified for the stimulation or poststimulation conditions (Table 3). Specifically, subjects in the JNJ-42165279 group relative to the placebo group showed greater activation during the anticipation condition but no significant differences during or after the breathing load. Mean BOLD Talairach-transformed percent signal changes in these five subregions of interest and estimated between-group differences based on results of the mixed effects ANOVA analysis are summarized in Supplementary Table 6 and shown in Fig. 2.

Fear conditioning task

RTs during each phase of the fear conditioning task are summarized in Supplementary Table 7. Values were similar between treatment groups and between phases, including the habituation period. After the habituation phase, the two acquisition phases, and at the end of the extinction phase, subjects verbally rated the CSs and how they were feeling using a VAS and a 5-point SAM (Supplementary Fig. 5). Results showed successful cued conditioning in both treatment groups. During the habituation phase, valence, arousal, and anxiety ratings for the CS− and the CS+ were similar. During the acquisition phase, ratings of negative valence, arousal, and anxiety were higher for the CS+ compared to the CS−. After extinction, CS+ and CS− ratings were similar to baseline (habituation) scores. There were no differences between the JNJ-42165279 and placebo treatment groups for ratings of valence or arousal to either cue type during the habituation, acquisition, or extinction phases and ratings of anxiety were similar between treatment groups during habituation.

Table 2. MRI emotional face-processing task—regions of interest: mean (SD) values and estimated treatment group differences (by condition and across conditions).

Subregion of interest	Condition	Placebo ($n = 20$) Mean (SD)	JNJ-42165279 ($n = 20$) Mean (SD)	LS mean Difference	p value[a]
ROI 1 (vol = 832 μL, $x = -23$, $y = -4$, $z = -14$, within left parahippocampal gyrus, BA 34)	Anger	0.463 (0.3393)	0.178 (0.4013)	−0.2853	0.0200*
	Fear	0.491 (0.5231)	0.037 (0.4608)	−0.4539	0.0060**
	Happy	0.511 (0.4675)	0.129 (0.2221)	−0.3815	0.0021**
	Across conditions	0.488 (0.4126)	0.115 (0.2876)	−0.3736	0.0020**
ROI 2 (vol = 1344 μL, $x = 15$, $y = 39$, $z = 12$, within right anterior cingulate, BA 32)	Anger	−0.029 (0.1292)	−0.130 (0.1529)	−0.1017	0.0288*
	Fear	−0.023 (0.2149)	−0.238 (0.2188)	−0.2158	0.0032**
	Happy	0.032 (0.1798)	−0.150 (0.1757)	−0.1820	0.0025**
	Across conditions	−0.006 (0.1570)	−0.173 (0.1481)	−0.1665	0.0014**
ROI 3 (vol = 960 μL, $x = -8$, $y = 36$, $z = -8$, within left medial frontal gyrus, BA 10)	Anger	0.009 (0.2812)	−0.249 (0.5379)	−0.2580	0.0650†
	Fear	0.112 (0.3438)	−0.415 (0.7263)	−0.5265	0.0057**
	Happy	0.208 (0.3778)	−0.261 (0.8177)	−0.4693	0.0252*
	Across conditions	0.110 (0.2765)	−0.308 (0.6660)	−0.4179	0.0135*
ROI 4 (vol = 896 μL, $x = -15$, $y = 38$, $z = 10$, within left anterior cingulate, BA 32)	Anger	−0.029 (0.1520)	−0.136 (0.2077)	−0.1073	0.0699†
	Fear	−0.038 (0.2046)	−0.312 (0.3960)	−0.2732	0.0093**
	Happy	0.046 (0.1671)	−0.136 (0.2636)	−0.1821	0.0129*
	Across conditions	−0.007 (0.1578)	−0.195 (0.2449)	−0.1875	0.0065*
ROI 5 (vol = 640 μL, $x = 12$, $y = 40$, $z = -8$, within right medial frontal gyrus, BA 10)	Anger	0.051 (0.3848)	−0.228 (0.4822)	−0.2796	0.0498*
	Fear	0.094 (0.5518)	−0.394 (0.6351)	−0.4876	0.0135*
	Happy	0.249 (0.3738)	−0.227 (0.6434)	−0.4765	0.0068**
	Across conditions	0.131 (0.3883)	−0.283 (0.5408)	−0.4146	0.0083**
ROI 6 (vol = 448 μL, $x = -39$, $y = -2$, $z = 14$, within left insula, BA 13)	Anger	0.099 (0.1990)	−0.100 (0.2214)	−0.1990	0.0049**
	Fear	0.037 (0.2990)	−0.087 (0.2649)	−0.1245	0.1715
	Happy	0.114 (0.2672)	−0.054 (0.1666)	−0.1673	0.0227*
	Across conditions	0.084 (0.2295)	−0.080 (0.1555)	−0.1636	0.0120*
ROI 7 (vol = 448 μL, $x = 36$, $y = -6$, $z = 15$, within right insula, BA 13)	Anger	0.158 (0.1396)	−0.055 (0.2763)	−0.2124	0.0040**
	Fear	0.130 (0.2730)	−0.131 (0.4877)	−0.2610	0.0435*
	Happy	0.108 (0.2028)	−0.016 (0.2325)	−0.1236	0.0810†
	Across conditions	0.132 (0.1824)	−0.067 (0.2811)	−0.1990	0.0115*

Numbers represent BOLD fMRI Talairach-transformed percent signal changes. Data represent averages over trials. Brain activity to shapes was subtracted. Across Conditions: for each subject, the average of the conditions was calculated and descriptive statistics were calculated based on these averages.
ROI region of interest, *BA* Brodmann's area.
†$p < 0.1$; *$p < 0.05$; **$p < 0.01$.
[a]Test for no difference between treatments from a mixed effects ANOVA model with condition (anger, fear, happy) as within-subject factor and treatment (placebo, JNJ-42165279) as between-subject factor.

Mean BOLD fMRI Talairach-transformed percent signal changes in the amygdala (the primary region of interest in this analysis) and other regions of interest (i.e., insula and anterior cingulate) during each phase of the fear conditioning task (habituation, two acquisition phases, and two extinction phases) represent the difference between percent signal changes during periods of conditioned stimulus (CS+) and during periods of unconditioned stimulus (CS−). Estimated between-group differences based on results of the mixed effects ANOVA analysis are summarized for each half of the acquisition and extinction phases in (Supplementary Table 8 and shown in Supplementary Fig. 5).

There were no subregions identified with a statistically significant difference between treatment groups, either during acquisition or extinction. To evaluate whether there was a task effect, contrasts were performed between the first and second half of extinction, collapsed across treatment groups, for CS+ vs. CS− values. Nine subregions were identified with statistically significant differences between the first and second half of extinction. For all subregions, activation was higher in the second half of extinction than the first half, however there was no group by time interaction.

DISCUSSION

This investigation using JNJ-42165279 in a 4-day administration study with healthy male volunteers to examine whether FAAH inhibition results in an anxiolytic profile based on three different fMRI tasks probing response to affect/arousal and interoception

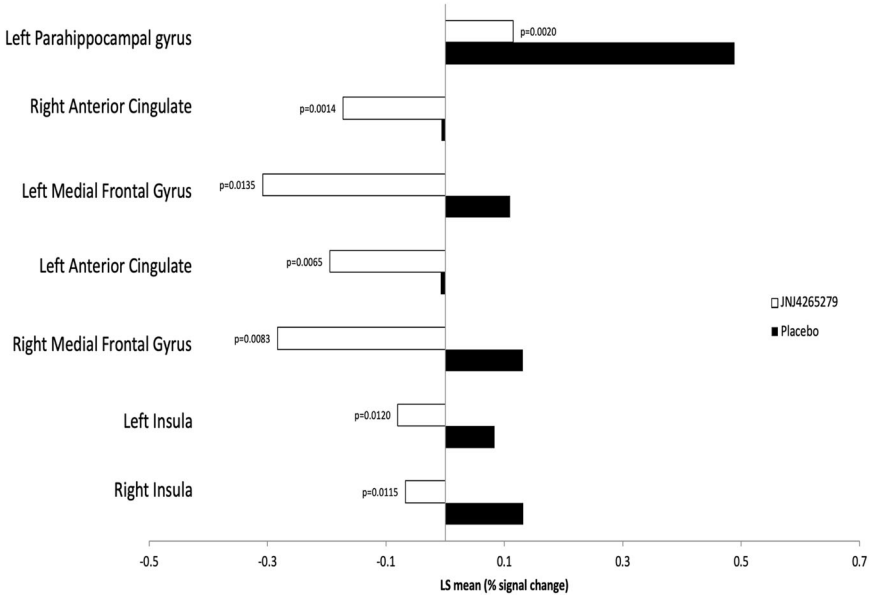

Fig. 1 MRI emotional face-processing task—regions of interest (across conditions): LS mean values. Numbers represent BOLD fMRI Talairach-transformed percent signal changes. Data represent averages over trials. Brain activity to shapes was subtracted. Volume (Vol) represents number of 4^3 uL voxels. Across conditions: for each subject, the average of the conditions was calculated; the LS mean is presented for these averages. *p* values based on test for no difference between treatments from a mixed effects ANOVA model with condition (anger, fear, happy) as within-subject factor and treatment (placebo, JNJ-42165279) as between-subject factor.

Table 3. MRI breathing load task—subregions of interest: mean (SD) values and estimated treatment group differences by condition.

Region	Condition	Placebo ($n = 20$) Mean (SD)	JNJ-42165279 ($n = 20$) Mean (SD)	LS mean Difference	*p* value[a]
Region of interest 1: vol = 1088 μL, $x = 5$, $y = 36$, $z = -9$, within right anterior cingulate, BA 32	Anticipation	−0.054 (0.1048)	0.087 (0.1176)	0.1405	0.0003**
	Stimulation	0.395 (0.4565)	0.286 (0.3141)	−0.1092	0.3838
	Post stimulation	1.055 (0.9650)	0.722 (0.7163)	−0.3330	0.2228
Region of interest 2: vol = 896 μL, $x = -39$, $y = 15$, $z = 0$, within left insula, BA 13	Anticipation	−0.004 (0.2367)	0.237 (0.3364)	0.2412	0.0125*
	Stimulation	0.076 (0.2767)	0.134 (0.3739)	0.0580	0.5806
	Post stimulation	0.271 (0.5902)	0.073 (0.5664)	−0.1978	0.2863
Region of interest 3: vol = 832 μL, $x = -36$, $y = -14$, $z = 18$, within left insula, BA 13	Anticipation	−0.038 (0.1241)	0.110 (0.2005)	0.1476	0.0080**
	Stimulation	0.537 (0.6773)	0.408 (0.3621)	−0.1293	0.4561
	Post stimulation	1.291 (1.5946)	0.970 (0.8224)	−0.3216	0.4277
Region of interest 4: vol = 1280 μL, $x = 50$, $y = -30$, $z = 18$, within right insula, BA 13	Anticipation	−0.052 (0.2098)	0.160 (0.2731)	0.2111	0.0093**
	Stimulation	0.254 (0.3334)	0.238 (0.2908)	−0.0154	0.8775
	Post stimulation	0.622 (0.6600)	0.515 (0.5187)	−0.1070	0.5721
Region of interest 5: vol = 448 μL, $x = 40$, $y = 20$, $z = 4$, within right inferior frontal gyrus, BA 45	Anticipation	0.065 (0.1969)	0.309 (0.3297)	0.2439	0.0072**
	Stimulation	0.568 (0.6727)	0.512 (0.4828)	−0.0561	0.7634
	Post stimulation	1.542 (1.4303)	1.295 (1.0594)	−0.2471	0.5384

Numbers represent BOLD fMRI Talairach-transformed percent signal changes. Data represent averages over trials.
**$p < 0.001$; *$p < 0.05$.
[a]Test for no difference between treatments from a mixed effects ANOVA model with condition (anticipation, stimulation, post stimulation) as within-subject factor and treatment (placebo, JNJ-42165279) as between-subject factor.

yielded three main results. First, JNJ-42165279 attenuated the activation in the amygdala, anterior cingulate, and bilateral insula during the face emotion processing task, consistent with effects previously observed with anxiolytic agents. Higher levels of plasma anandamide were associated with greater attenuation in these brain areas. Second, JNJ-42165279 increased the activation during anticipation of an aversive interoceptive event in the anterior cingulate and bilateral anterior insula. Third, JNJ-42165279 did not affect acquisition or within-session extinction learning of a conditioned stimulus paired with an aversive unconditioned stimulus on a subjective or neural circuit level. Taken together, these results are consistent with the hypothesis that JNJ-42165279 shares some effects with existing anxiolytic agents such as benzodiazepines but does not affect fear conditioning or within-session fear extinction learning.

Animal studies have implicated several brain areas for the eCB modulation of stress. Chronic stress significantly reduces the content of the eCB 2-arachidonylglycerol within the hippocampus [58]. Other studies indicate that CB1 receptors in the mPFC and ventral hippocampus appear to be responsible for the

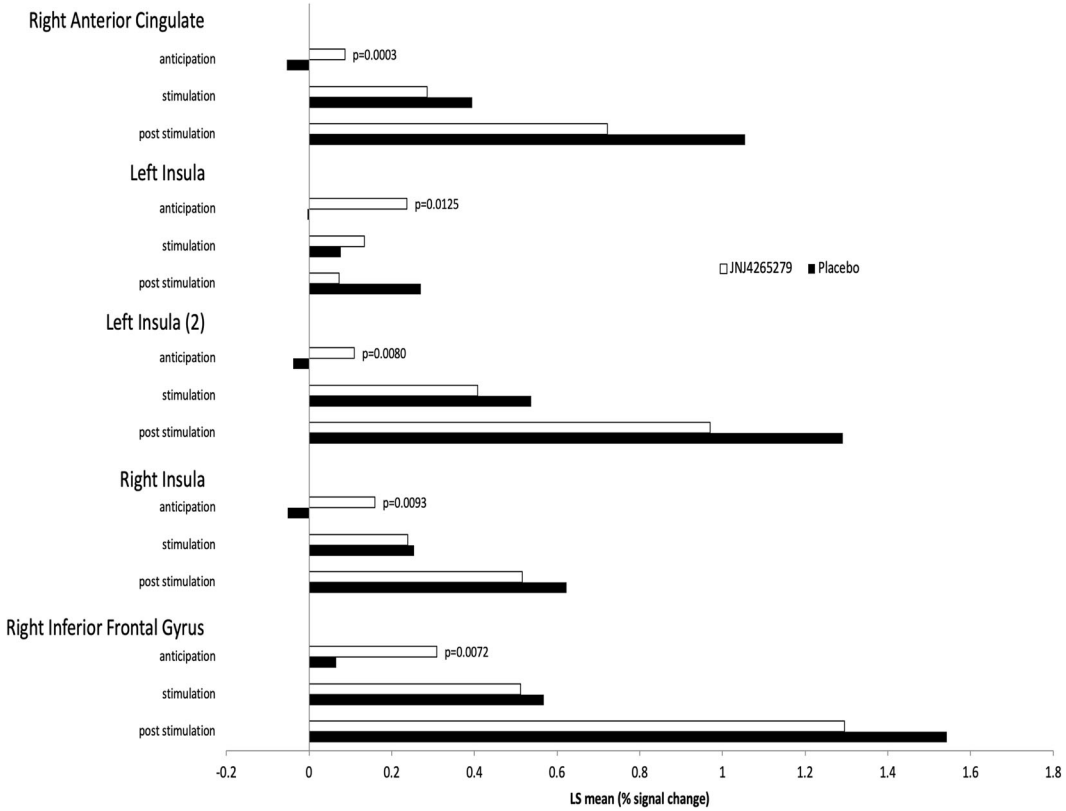

Fig. 2 MRI breathing load task—subregions of interest (by condition): LS mean values. Numbers represent BOLD fMRI Talairach-transformed percent signal changes. Data represent averages over trials. *p* values are based on test for no difference between treatments from a mixed effects ANOVA model with condition as within-subject factor and treatment (placebo, JNJ-42165279) as between-subject factor.

antidepressant- and anxiolytic-like effects of AEA [14]. Moreover, reductions of CB1 receptor activation within the basolateral amygdala and central amygdala promote anxiogenesis and anxiolysis, respectively [59]. Finally, local inhibition of anandamide hydrolysis within the medial PFC increases the firing rate of serotonergic neurons suggesting that prefrontal cortical eCB signaling may modulate stress coping behaviors through regulation of serotonergic neurotransmission [60]. We found that FAAH inhibition during both face emotion processing and during inspiratory breathing load involved some of the brain areas that have been implicated by animal studies. In particular, the mPFC, including the anterior cingulate, is important for modulating bottom up emotional processes. There is some evidence from previous studies that highly resilient individuals show greater anticipatory brain responses to aversive interoceptive stimuli [47]. Thus, the combination of attenuation during facial processing and increased activation during the anticipation of aversive events is consistent with the notion that FAAH inhibition may have two different effects on negatively valenced stimuli: attenuating the emotional impact of emotional faces and increasing the top-down preparation for impending aversive events when the individual is afforded an anticipatory period.

There is strong evidence from animal studies that CB1 signaling modulates learned fear processes, in particular fear extinction [8]. Effects of CB1 signaling on fear expression are less consistent than effects on extinction [13], with modulation of fear expression requiring specific cortical CB1 receptor circuits [61, 62]. In rodents, FAAH inhibition may also be more effective at blocking contextual fear vs. cued fear [63, 64]. FAHH inhibition has most consistently been shown to enhance 24-h recall of extinction in rodents, either systemically or when inhibitors are administered selectively in the hippocampus or basolateral amygdala [65, 66]. This selective enhancement of extinction recall with minimal effects on fear conditioning or extinction learning after FAAH inhibition has also recently been replicated in a human fear conditioning paradigm [16] after 10 days of treatment. In the present study, JNJ-42165279 had no observable effects on fear acquisition or extinction learning after 4 days of treatment. Although a fear conditioning and extinction paradigm which has been developed to maximize activation of the relevant neural circuitry was used [45], there was no explicit examination of consolidation, which would have necessitated a second day of testing. In contrast to our findings that relatively acute increases in AEA do not affect within-session learning, lifetime increases in AEA due to genetic mutations in the FAAH gene are associated with increased within-session extinction learning [67]. These different findings may be due to developmental effects of long-term AEA abundance. Future studies should examine the effects of JNJ-42165279 on extinction recall. There is also some recent evidence that modulating the eCB system may result in an inverted U-shaped dose response for anxiety in humans. Thus, a dose response study may help to further clarify the role of this system in human fear conditioning and extinction.

This study has several limitations. First, JNJ-42165279 did not affect subjective assessments, i.e., symptoms of stress or anxiety, in these healthy volunteers. Therefore, this study was unable to connect the subjective unit of analysis to neural circuits. Second, this study was not designed to compare the differences between acute and chronic effects of JNJ-42165279, which may have shed light on adaptive changes that contribute to the possible therapeutic effects of this drug. Third, this study was conducted with healthy male volunteers, who may have a different subjective and circuit level baseline than women particularly as it relates to fear learning [68]. Moreover, target (patient) populations may show different emotion-related processing effects than healthy volunteers that could be affected by FAAH inhibition. Nevertheless, prior studies using this pharmaco-fMRI approach have

shown that brain activation changes to other psychoactive agents are similar in healthy volunteers and target populations [69, 70]. Therefore, future investigations should focus on acute and chronic administration of FAAH inhibitors and their effect on stress and fear related processing in healthy volunteers as well as target populations such as patients with PTSD. Fourth, this study focused on within-session extinction and did not include a multi-session fear extinction session [71], which may be necessary to better examine the effects of FAAH inhibition on extinction learning.

In conclusion, this study was aimed to examine whether steady-state inhibition of FAAH, which enhances the effect of the eCB system that is important for stress regulation, showed an anxiolytic-like profile on neural circuits in healthy volunteers. The results are partially consistent with the hypothesis that FAAH helps to process negative valenced information possibly by augmenting processing of anticipatory modulation of upcoming events. However, there was no evidence for modulation of fear conditioning or within-session extinction. Comparing these results to prior studies with known anxiolytic agents suggests that FAAH inhibition might have a role in treating individuals with anxiety and stress-related disorders.

FUNDING AND DISCLOSURE

This work has been supported by Janssen Research & Development. In addition, MPP is supported by The William K. Warren Foundation, the National Institute on Drug Abuse (U01 DA041089), and the National Institute of General Medical Sciences Center Grant Award Number (1P20GM121312). The content is solely the responsibility of the authors and does not necessarily represent the official views of the National Institutes of Health. VBR and ANS are supported by the VA Center of Excellence for Stress and Mental Health and via VA BLR&D and CSR&D Merit awards respectively. MPP is an advisor to Spring Care, Inc., a behavioral health startup, he has received royalties for an article about methamphetamine in UpToDate. VBR and ANS have nothing to disclose. MBS has in the past 3 years been a consultant for Acadia, Aptinyx, Bionomics, Epivario, GW Pharmaceuticals, Janssen, and Oxeia Biopharmaceuticals. RH is an employee of Janssen Research & Development, LLC, San Diego, California. Janssen is developing JNJ-42165279 for treatments in mood and anxiety disorders. SRC is an employee of Janssen Research & Development, LLC, San Diego, California. Janssen is developing JNJ-42165279 for treatments in mood and anxiety disorders.

ACKNOWLEDGEMENTS

We would like to thank Ilse Van Hove, MSc, for statistical advice and support in preparing this manuscript.

AUTHOR CONTRIBUTIONS

MPP, MBS, ANS, VBR, RH, and SRC were involved in the planning of the study. MPP, MBS, ANS, and VBR were involved in the collection of the data. MPP, MBS, ANS, and VBR were involved in analyzing the data. MPP, MBS, ANS, VBR, RH, and SRC substantially contributed to writing the manuscript.

ADDITIONAL INFORMATION

Supplementary Information accompanies this paper at (https://doi.org/10.1038/s41386-020-00936-w).

Publisher's note Springer Nature remains neutral with regard to jurisdictional claims in published maps and institutional affiliations.

REFERENCES

1. Kessler RC, McGonagle KA, Zhao S, Nelson CB, Hughes M, Eshleman S, et al. Lifetime and 12-month prevalence of DSM-III-R psychiatric disorders in the United States. Results from the National Comorbidity Survey. Arch Gen Psychiatry. 1994;51:8–19.
2. Kessler RC, Petukhova M, Sampson NA, Zaslavsky AM, Wittchen HU. Twelve-month and lifetime prevalence and lifetime morbid risk of anxiety and mood disorders in the United States. Int J Methods Psychiatr Res. 2012;21:169–84.
3. Baxter AJ, Vos T, Scott KM, Ferrari AJ, Whiteford HA. The global burden of anxiety disorders in 2010. Psychol Med. 2014;44:1–12.
4. Loerinc AG, Meuret AE, Twohig MP, Rosenfield D, Bluett EJ, Craske MG. Response rates for CBT for anxiety disorders: Need for standardized criteria. Clin Psychol Rev. 2015;42:72–82.
5. Stein MB, Craske MG. Treating anxiety in 2017: optimizing care to improve outcomes. JAMA. 2017;318:235–36.
6. Riebe CJ, Wotjak CT. Endocannabinoids and stress. Stress. 2011;14:384–97.
7. Morena M, Patel S, Bains JS, Hill MN. Neurobiological interactions between stress and the endocannabinoid system. Neuropsychopharmacology. 2016;41:80–102.
8. Lutz B, Marsicano G, Maldonado R, Hillard CJ. The endocannabinoid system in guarding against fear, anxiety and stress. Nat Rev Neurosci. 2015;16:705–18.
9. Jafarpour A, Dehghani F, Korf HW. Identification of an endocannabinoid system in the rat pars tuberalis-a possible interface in the hypothalamic-pituitary-adrenal system? Cell Tissue Res. 2017;368:115–23.
10. Korem N, Zer-Aviv TM, Ganon-Elazar E, Abush H, Akirav I. Targeting the endocannabinoid system to treat anxiety-related disorders. J basic Clin Physiol Pharmacol. 2016;27:193–202.
11. Bluett RJ, Gamble-George JC, Hermanson DJ, Hartley ND, Marnett LJ, Patel S. Central anandamide deficiency predicts stress-induced anxiety: behavioral reversal through endocannabinoid augmentation. Transl Psychiatry. 2014;4:e408.
12. Hill MN, Kumar SA, Filipski SB, Iverson M, Stuhr KL, Keith JM, et al. Disruption of fatty acid amide hydrolase activity prevents the effects of chronic stress on anxiety and amygdalar microstructure. Mol Psychiatry. 2013;18:1125–35.
13. Gunduz-Cinar O, Hill MN, McEwen BS, Holmes A. Amygdala FAAH and anandamide: mediating protection and recovery from stress. Trends Pharmacol Sci. 2013;34:637–44.
14. Lisboa SF, Borges AA, Nejo P, Fassini A, Guimaraes FS, Resstel LB. Cannabinoid CB1 receptors in the dorsal hippocampus and prelimbic medial prefrontal cortex modulate anxiety-like behavior in rats: additional evidence. Prog Neuropsychopharmacol Biol Psychiatry. 2015;59:76–83.
15. Kathuria S, Gaetani S, Fegley D, Valino F, Duranti A, Tontini A, et al. Modulation of anxiety through blockade of anandamide hydrolysis. Nat Med. 2003;9:76–81.
16. Mayo LM, Asratian A, Linde J, Morena M, Haataja R, Hammar V, et al. Elevated anandamide, enhanced recall of fear extinction, and attenuated stress responses following inhibition of fatty acid amide hydrolase: a randomized, controlled experimental medicine trial. Biol Psychiatry. 2020;87:538–47.
17. Kinsey SG, O'Neal ST, Long JZ, Cravatt BF, Lichtman AH. Inhibition of endocannabinoid catabolic enzymes elicits anxiolytic-like effects in the marble burying assay. Pharm Biochem Behav. 2011;98:21–7.
18. Rabinak CA, Phan KL. Cannabinoid modulation of fear extinction brain circuits: a novel target to advance anxiety treatment. Curr Pharm Des. 2014;20:2212–7.
19. Howlett JR, Stein MB. Prevention of trauma and stressor-related disorders: a review. Neuropsychopharmacology 2016;41:357–69.
20. Patel S, Hill MN, Cheer JF, Wotjak CT, Holmes A. The endocannabinoid system as a target for novel anxiolytic drugs. Neurosci Biobehav Rev. 2017;76:56–66.
21. Insel TR. Next-generation treatments for mental disorders. Sci Transl Med. 2012;4:155ps19.
22. Cuthbert BN, Insel TR. Toward the future of psychiatric diagnosis: the seven pillars of RDoC. BMC Med. 2013;11:126.
23. Health NIoM. Positive Valence Systems: Workshop Proceedings. 2011. http://www.nimh.nih.gov/research-funding/rdoc/positive-valence-systems-workshop-proceedings.shtml. Accessed 10 Dec 2012.
24. Health NIoM. Negative Valence Systems: Workshop Proceedings. 2011. http://www.nimh.nih.gov/research-funding/rdoc/negative-valence-systems-workshop-proceedings.shtml. Accessed 10 Dec 2012.
25. Bouton ME, King DA. Contextual control of the extinction of conditioned fear: tests for the associative value of the context. J Exp Psychol Anim Behav Process. 1983;9:248–65.
26. Griez E. Experimental models of anxiety. Problems and perspectives. Acta Psychiatr Belg. 1984;84:511–32.
27. Davis M. Pharmacological and anatomical analysis of fear conditioning using the fear-potentiated startle paradigm. Behav Neurosci. 1986;100:814–24.
28. Phillips RG, LeDoux JE. Differential contribution of amygdala and hippocampus to cued and contextual fear conditioning. Behav Neurosci. 1992;106:274–85.
29. Labar KS, Gatenby JC, Gore JC, LeDoux JE, Phelps EA. Human amygdala activation during conditioned fear acquisition and extinction: a mixed-trial fMRI study. Neuron 1998;20:937–45.
30. Buchel C, Dolan RJ. Classical fear conditioning in functional neuroimaging. Curr Opin Neurobiol. 2000;10:219–23.

31. Delgado MR, Olsson A, Phelps EA. Extending animal models of fear conditioning to humans. Biol Psychol. 2006;73:39–48.
32. Etkin A, Wager TD. Functional neuroimaging of anxiety: a meta-analysis of emotional processing in PTSD, social anxiety disorder, and specific phobia. Am J Psychiatry. 2007;164:1476–88.
33. Hariri AR, Tessitore A, Mattay VS, Fera F, Weinberger DR. The amygdala response to emotional stimuli: a comparison of faces and scenes. Neuroimage 2002;17:317–23.
34. Fonzo GA, Ramsawh HJ, Flagan TM, Sullivan SG, Letamendi A, Simmons AN, et al. Common and disorder-specific neural responses to emotional faces in generalised anxiety, social anxiety and panic disorders. Br J Psychiatry. 2015;206:206–15.
35. Paulus MP, Feinstein JS, Castillo G, Simmons AN, Stein MB. Dose-dependent decrease of activation in bilateral amygdala and insula by lorazepam during emotion processing. Arch Gen Psychiatry. 2005;62:282–8.
36. Paulus MP, Stein MB. An insular view of anxiety. Biol Psychiatry. 2006;60:383–7.
37. Craig AD. How do you feel? Interoception: the sense of the physiological condition of the body. Nat Rev Neurosci. 2002;3:655–66.
38. Craig AD. How do you feel—now? The anterior insula and human awareness. Nat Rev Neurosci. 2009;10:59–70.
39. Vaitl D. Interoception. Biol Psychol. 1996;42:1–27.
40. Augustine JR. Circuitry and functional aspects of the insular lobe in primates including humans. Brain Res Brain Res Rev. 1996;22:229–44.
41. Craig AD. Interoception and Emotion: a Neuroanatomical Perspective. In: Lewis M, Haviland-Jones JM, Feldman Barrett L, eds. Handbook of Emotions. New York, NY: Guilford Press; 2007. p. 272–90.
42. Andrade AK, Renda B, Murray JE. Cannabinoids, interoception, and anxiety. Pharm Biochem Behav. 2019;180:60–73.
43. Keith JM, Jones WM, Tichenor M, Liu J, Seierstad M, Palmer JA, et al. Preclinical characterization of the FAAH inhibitor JNJ-42165279. ACS Med Chem Lett. 2015;6:1204–8.
44. Stewart JL, Parnass JM, May AC, Davenport PW, Paulus MP. Altered fronto-cingulate activation during aversive interoceptive processing in young adults transitioning to problem stimulant use. Front Syst Neurosci. 2013;7:89.
45. Sehlmeyer C, Dannlowski U, Schoning S, Kugel H, Pyka M, Pfleiderer B, et al. Neural correlates of trait anxiety in fear extinction. Psychol Med. 2011;41:789–98.
46. Hariri AR, Mattay VS, Tessitore A, Kolachana B, Fera F, Goldman D, et al. Serotonin transporter genetic variation and the response of the human amygdala. Science. 2002;297:400–03.
47. Paulus MP, Flagan T, Simmons AN, Gillis K, Kotturi S, Thom N, et al. Subjecting elite athletes to inspiratory breathing load reveals behavioral and neural signatures of optimal performers in extreme environments. PLoS One. 2012;7:e29394.
48. Sehlmeyer C, Schoning S, Zwitserlood P, Pfleiderer B, Kircher T, Arolt V, et al. Human fear conditioning and extinction in neuroimaging: a systematic review. PloS one. 2009;4:e5865.
49. Cox RW. AFNI: software for analysis and visualization of functional magnetic resonance neuroimages. Comput Biomed Res. 1996;29:162–73.
50. Haxby JV, Petit L, Ungerleider LG, Courtney SM. Distinguishing the functional roles of multiple regions in distributed neural systems for visual working memory [see comments]. Neuroimage 2000;11:380–91.
51. Eddy WF, Fitzgerald M, Noll DC. Improved image registration by using Fourier interpolation. Magn Reson Med. 1996;36:923–31.
52. Ball TM, Knapp SE, Paulus MP, Stein MB. Brain activation during fear extinction predicts exposure success. Depress Anxiety. 2017;34:257–66.
53. Boynton GM, Engel SA, Glover GH, Heeger DJ. Linear systems analysis of functional magnetic resonance imaging in human V1. J Neurosci. 1996;16:4207–21.
54. Friston KJ, Frith CD, Turner R, Frackowiak RS. Characterizing evoked hemodynamics with fMRI. Neuroimage. 1995;2:157–65.
55. Cohen MS. Parametric analysis of fMRI data using linear systems methods. Neuroimage. 1997;6:93–103.
56. Pinheiro JB, D; DebRoy, S; Sarkar, D. Linear and Nonlinear Mixed Effects Models. http://CRAN.R-project.org/package=nlme (2016).
57. R: A Language and Environment for Statistical Computing. R Foundation for Statistical Computing: Vienna, Austria; 2010.
58. Hill MN, Patel S, Carrier EJ, Rademacher DJ, Ormerod BK, Hillard CJ, et al. Downregulation of endocannabinoid signaling in the hippocampus following chronic unpredictable stress. Neuropsychopharmacology. 2005;30:508–15.
59. McLaughlin RJ, Gobbi G. Cannabinoids and emotionality: a neuroanatomical perspective. Neuroscience. 2012;204:134–44.
60. McLaughlin RJ, Hill MN, Bambico FR, Stuhr KL, Gobbi G, Hillard CJ, et al. Prefrontal cortical anandamide signaling coordinates coping responses to stress through a serotonergic pathway. Eur Neuropsychopharmacol. 2012;22:664–71.
61. Busquets-Garcia A, Desprez T, Metna-Laurent M, Bellocchio L, Marsicano G, Soria-Gomez E. Dissecting the cannabinergic control of behavior: the where matters. Bioessays. 2015;37:1215–25.
62. Morena M, Aukema RJ, Leitl KD, Rashid AJ, Vecchiarelli HA, Josselyn SA, et al. Upregulation of anandamide hydrolysis in the basolateral complex of amygdala reduces fear memory expression and indices of stress and anxiety. J Neurosci. 2019;39:1275–92.
63. Vimalanathan A, Gidyk DC, Diwan M, Gouveia FV, Lipsman N, Giacobbe P, et al. Endocannabinoid modulating drugs improve anxiety but not the expression of conditioned fear in a rodent model of post-traumatic stress disorder. Neuropharmacology. 2020;166:107965.
64. Burman MA, Szolusha K, Bind R, Kerney K, Boger DL, Bilsky EJ. FAAH inhibitor OL-135 disrupts contextual, but not auditory, fear conditioning in rats. Behav Brain Res. 2016;308:1–5.
65. Segev A, Korem N, Mizrachi Zer-Aviv T, Abush H, Lange R, Sauber G, et al. Role of endocannabinoids in the hippocampus and amygdala in emotional memory and plasticity. Neuropsychopharmacology. 2018;43:2017–27.
66. Gunduz-Cinar O, MacPherson KP, Cinar R, Gamble-George J, Sugden K, Williams B, et al. Convergent translational evidence of a role for anandamide in amygdala-mediated fear extinction, threat processing and stress-reactivity. Mol Psychiatry. 2013;18:813–23.
67. Dincheva I, Drysdale AT, Hartley CA, Johnson DC, Jing D, King EC, et al. FAAH genetic variation enhances fronto-amygdala function in mouse and human. Nat Commun. 2015;6:6395.
68. Lebron-Milad K, Abbs B, Milad MR, Linnman C, Rougemount-Bucking A, Zeidan MA, et al. Sex differences in the neurobiology of fear conditioning and extinction: a preliminary fMRI study of shared sex differences with stress-arousal circuitry. Biol Mood Anxiety Disord. 2012;2:7.
69. Harmer CJ, Mackay CE, Reid CB, Cowen PJ, Goodwin GM. Antidepressant drug treatment modifies the neural processing of nonconscious threat cues. Biol Psychiatry. 2006;59:816–20.
70. Di Simplicio M, Norbury R, Harmer CJ. Short-term antidepressant administration reduces negative self-referential processing in the medial prefrontal cortex in subjects at risk for depression. Mol Psychiatry. 2012;17:503–10.
71. Schiller D, Monfils MH, Raio CM, Johnson DC, Ledoux JE, Phelps EA. Preventing the return of fear in humans using reconsolidation update mechanisms. Nature 2010;463:49–53.